KOREAN JOURNAL OF PACKAGING SCIENCE & TECHNOLOGY
Vol. 24, No. 3 149~157 (2018)
https://doi.org/10.20909/kopast.2018.24.3.149

Effect of Carbon Dioxide Adsorption on LDPE/Zeolite 4A Composite Film

Bich Nam Jung[1,2], Jin Kie Shim[1], and Sung Wook Hwang[1]*

[1]Korea Packaging Center, Korea Institute of Industrial Technology, Bucheon, Korea
[2]Department of Chemical and Biological Engineering, Korea University, Seoul, Korea

Abstract Low density polyethylene (LDPE) has been researched in many industrial applications, and LDPE/zeolite 4A composites has been extensively studied for many applications such as microporous, breathable film and so on. LDPE/zeolite composite have a great potential for carbon dioxide adsorption film due to its high adsorption ability. In this study, LDPE/zeolite 4A composites with various contents were prepared by melt mixing process, and co-extrusion process was applied to develop a CO_2 adsorption conventional film and foamed film. The thermal, rheological, mechanical, physical and morphological properties of composite films has been characterized, and CO_2 adsorption of the composite films evaluated by thermogravimetric analysis (TGA) and the performance was found to be about 18 cc/g at 30.9 wt% of the zeolite content.

Keywords LDPE, Zeolite 4A, Carbon dioxide adsorption, Composite, Film, Foaming

Introduction

Low-density polyethylene (LDPE) as packaging plastic material has been widely used for its excellent properties such as low cost, flexibility, chemical resistance, and easy processability. However, LDPE itself is not welcomed in food packaging application due to improper poor food conservation ability and could not guarantee the long shelf life of the contained food products. Therefore, various multi-layer structures and composite materials has been widely applied to the field of food packaging to keep the freshness during the distribution and consumption.

One of the most important functions for food packaging materials is preventing food quality deterioration from the various environmental influences[1]. Among them, carbon dioxide (CO_2) is one of the factors to be considered to design the packaging for food products. Daniels et al.[2] reported CO_2 is effective in delaying bacterial growth and thus prolonging the shelf life of perishable foods. Some studies show that 20~30% CO_2 concentration is sufficient to prevent the growth of aerobic bacteria[3]. In addition, according Luno et al.[4] the high concentration of CO_2 is easily oxidized leading to loss of fresh color and odor of the products. Therefore, the research for the packaging materials having an ability of CO_2 adsorption is necessary to extend the shelf life of products generating CO_2 such as fresh-roasted ground coffee and fermented foods.

Polymer composite combining the polymer with micro/nano scaled inorganic fillers to develop the materials with better performance is good option to solve the limitations of the polymers for a variety of industrial applications[5]. The inorganic fillers having CO_2 adsorbing ability include zeolite[6-9], activated carbon[10], graphene oxide[11], carbon nanotube[12] and so on. Previous researches have shown that various zeolites exhibit the higher CO_2 adsorption performance than carbon-based fillers such as activated carbon[13,14]. Furthermore, Siriwardane et al.[14] measured the adsorption of CO_2, N_2, H_2 and their mixtures on zeolite, and it was found that CO_2 was selectively adsorbed to these zeolites for N_2 and H_2 over a wide range of pressures at room temperature. In this study, zeolite 4A having micro-pores of approximately 3.8 Å was selected as a filler considering that the kinetic diameter of CO_2 is 3.3 Å.

The purpose of the active packaging system is to improve the quality of food and extend its shelf life, and is normally prepared with direct incorporation of active substance to the polymer making the packaging film[15].

In recent years, the cellular foam structures in polymer composites through a continuous extrusion foaming process has been successfully proved to enhance the performance of composites[16-18]. By foaming the polymer composite, the lower density was accomplished which is good for industrial appli-

†Corresponding Author : Sung Wook Hwang
Korea Packaging Center, Korea Institute of Industrial Technology, Bucheon, Korea
Tel : +82-32-624-4758, Fax : +82-
E-mail : swhwang@kitech.re.kr

cations, and the micro-structure of foamed cells within the polymer composite could affect the performance of the inorganic filler during the melt pocesssing.

Several techniques have been applied to prepare polymer/zeolite composites such as solution casting[19-23], in-situ[24-26], and melt processing[27-29]. LDPE/zeolite 4A composites have been researched exclusively in microporous and breathable films for packaging application[29].

To the best of author's knowledge, no study was found to characterize the compounding of LDPE and zeolite 4A with respect to the CO_2 adsorption property. In this study, LDPE/zeolite 4A composite master batches with various contents (9.6, 16.3, 25.2 and 30.9 wt%) were prepared by melt mixing process. In addition, the master batch was continuous extruded in the form of a film using a flat dies and was also prepared foamed film with a chemical blowing agent. The thermal, rheological, mechanical, physical and morphological properties of composites has been characterized, and the CO_2 adsorption of the composite films was assessed by thermogravimetric analysis (TGA).

Materials and Methods

1. Materials

LDPE (BS500 grade, melt index: 3.3 g/10 min, 190°C 2.16 kg ASTM D1238) was obtained from LG chemical (Korea). The zeolite 4A [COLITE-P] was purchased from the Cosmo fine chemicals (Korea). COLITE-P has the molecular formula of $Na_{12}[(AlO_2)\cdot(SiO_2)]_{12}\cdot 27H_2O$, and the average particle size is 2.0 to 3.5 microns. Chemical Blowing agent [CELLCOM-ACMP, decomposition temperature: 193~197°C], azodicarbonamide series, was provided by the Kum yang (Korea). All of the additives were vacuum-dried at 80°C for 12 hrs to remove residual moisture before use.

2. Methods

1) Sample preparation

A Brabender microcompounder TSC 42/6 (Brabender, Duisburg, Germany) designed with a small scale conical, counter-rotating twin-screw compounder with a screw diameter of 42 mm (L/D = 6) was used. LDPE/zeolite 4A composite master batches (MB series) with various compositions (10~40 wt%) were produced under barrel temperature at 200°C with a rotation speed at 50 rpm.

After pelletizing, the residual amount of fillers in composite was analyzed using thermogravimetric analyzer (TGA) (Model: Q500, TA Instruments, USA). After dried at 80°C for 12 hrs, the composites were also injection molded for measuring rheological properties at 200°C using a Xplore Micro Injection Moulding Machine (Xplore Instruments, Geleen, Netherlands) into test specimen with a disk shape of 25.4 mm diameter and 1 mm thickness. Then LDPE/zeolite 4A composite films (F series) were prepared under barrel temperature at 200 °C with a rotation speed at 25 rpm. Foaming films (FF series) with 10 phr of a blowing agent were also extruded continuously through the same conditions. In order to evaluate the physical properties of the two types of films, they were maintained at a thickness of about 200~350 μm.

3. Thermal measurement

The residual amount of master batch and film samples was observed by thermogravimetric analysis (Model: Q500, TA Instruments, USA). The tests were performed under a nitrogen atmosphere at temperatures of up to 600°C at a 10°C/min heating rate.

Thermal properties, including crystallinity and melting temperature of the master batches were analyzed by differential scanning calorimetry (Model: Q2000, TA Instruments, USA). The samples were placed in packed aluminum pan and then heated and cooled from 20 to 200°C, using a heating and cooling rate of 5°C/min. In order to estimate the X_c, the following equation was used:

$$X_c = \frac{\Delta H}{\Delta H_{100}(1-\phi)} \times 100 \quad (1)$$

Where ΔH the heat of fusion at melting point of the sample is analyzed [J/g] and ΔH_{100} is a reference value that represents the heat of fusion for a 100% α-crystalline polymer. For PE, ΔH_{100} is 288 J/g, and ϕ is the weight fraction of fillers[30].

4. Rheological measurement

Oscillatory shear measurement and stress relaxation in the linear viscoelastic (LVE) region were carried out which an Anton Paar rotational rheometer (Model: Physical MCR 302, Anton Paar GmbH, Austria) using parallel plates geometry (diameter 25 mm and measuring gap 1 mm) at 200°C. Frequency sweeps were performed after approximately 2 min temperature equilibration with decreasing frequency from 100 to 0.1 rad/s and strains at 1%.

5. Mechanical measurement

The mechanical properties such as tensile strength, young's modulus and elongation at break were tested on an INSTRON 3367 (INSTRON, MA, USA) equipped with 1 kN cell force, measuring force over displacement for each sample at 50 mm/min according to ASTM D 638. The sample were cut into dumbbell shape with dimensions of type IV specimen (width overall: 19 mm, length overall: 115 mm). At least 5 samples were tested for each film sample.

6. Physical measurement

The relative density of the composite films and foaming films are analyzed using a MD-300S densimeter (MIRAGE, Japan) following the water displacement method. According

to ASTM D792, the density of a sample (ρ_{exp}) is calculated by Eq. (2):

$$\rho_{exp} = \frac{\alpha}{\alpha - \beta} \times \rho_{water} \quad (2)$$

Where α is the apparent mass of the sample in air, β is the apparent mass of the sample completely immersed in water, and ρ_{water} is the density of distilled water at 23°C. Theoretical densities of foaming films (ρ_{th}) are calculated using the standard rule of mixtures (Eq. (3)):

$$\rho_{th} = \rho_{zeolite}\phi_{zeolite} + \rho_{matrix}\phi_{matrix} + \rho_{cell}\phi_{cell} \quad (3)$$

Where ρ and ϕ represent density and volume fraction, respectively, and the subscripts zeolite, matrix and cell describe zeolite 4A, polymer matrix and foam cell, respectively. Density of polymer matrix (LDPE) and zeolite 4A is 0.92 and 0.30 g/cm^3, respectively. The theoretical and experimental density (ρ_{exp}) are compared and the foam cell porosity trapped in the polymer matrix (ϕ_{cell}) during foaming process is calculated by Eq. (4):

$$\phi_{cell} = \frac{\rho_{th} - \rho_{exp}}{\rho_{th}} \quad (4)$$

7. Morphological measurement

The morphology of extruded samples was observed with a field emission scanning electron microscope (Model: SU8020, Hitachi, Japan). Samples was sectioned cross-section using a diamond knife in a freezing ultramicrotome (Model: LEICA ULTRACUT UC7, Leica, Germany). All of the cross sections were coated with Pt/Pd alloy using ion sputter (Model: E-1045, Hitachi, Japan), and measurement was performed under high vacuum with the acceleration voltage of 5 to 10 kV.

8. Carbon dioxide adsorption measurement

The CO_2 adsorption properties of film samples was tested with a thermogravimetric analysis (Model: Q500, TA Instruments, USA). Films was loaded at sample pan in the furnace. And dried under a nitrogen atmosphere until the weight change equilibrium at 75°C to remove residual moisture in the film. Thereafter, the temperature was cooled to 30°C and CO_2 was injected to measure the amount of CO_2 adsorption. At this time, the balance gas is injected at a flow rate of 10 ml/min with nitrogen, and the sample gas is injected at 90 ml/min with CO_2. Likewise, the weight change was measured until equilibrium was reached. CO_2 and nitrogen used 99% high purity gas.

The adsorption amount per unit mass of sample (M_{ads}) is calculated by Eq. (5):

$$M_{ads} = \frac{M_{inc}}{M_{sam}} \quad (5)$$

Where M_{sam} is the sample mass after moisture removal, M_{inc} is the sample mass increase after adsorption. The volume of CO_2 adsorption to the sample mass at 30°C and 1 atm (V_{ads}) is calculated by Eq. (6):

$$V_{ads} = \frac{M_{ads}}{\rho_{CO_2,\,30°C,\,1atm}} \quad (6)$$

Where $\rho_{CO_2,\,30°C,\,1atm}$ is the density of CO_2 at a temperature of 30°C and a pressure of 1 atm.

Results & Discussion

1. Thermal properties

Table 1 presents the results of thermal properties obtained from TGA. Zeolite 4A is well known for its ability to adsorb CO_2 due to physical or chemical adsorption[31]. In preparing LDPE/zeolite 4A composite master batches, zeolite 4A was added to LDPE in various contents ranging from 10 to 40 wt%. However, as a result of TGA, there was a slight difference between the actually injected amount and the difference was larger as the content of zeolite 4A increased. This is due to losses in the extruder during melt processing. Whereas, no loss occurred when extruding the film and the foaming film using the composite master batches, and there was marginal difference in content between the master batch content and the two types of films.

Table 2 shows the DSC results of LDPE/zeolite 4A composites with different zeolite 4A content. Compared with neat LDPE, LDPE/zeolite 4A composites with varying amount of zeolite 4A content showed no difference in melting temperature. The values of the heat of fusion shown in Table 2 were lower than those of neat LDPE. This could be due to the increase of the filler content of the composite, and the decrease of the heat of fusion could be attributed to the reduction of the

Table 1. The results of thermal properties of LDPE/zeolite 4A composites, films and foaming films with varying amount of zeolite 4A content

Sample Code	Residue amounts (wt%)
MB10	9.59 ± 0.12
10F	9.15 ± 0.17
10FF	9.46 ± 0.08
MB16	16.28 ± 0.19
16F	14.79 ± 0.43
16FF	15.23 ± 0.67
MB25	25.23 ± 0.60
25F	24.62 ± 0.16
25FF	23.54 ± 0.51
MB31	30.86 ± 0.98
31F	31.81 ± 0.08
31FF	29.36 ± 0.13

Table 2. The results of differential scanning calorimetry of LDPE/zeolite 4A composites with varying amount of zeolite 4A content

Sample Code	Melting temperature T_m (°C)	Heat of fusion at melting point ΔH (J/g)	Crystallinity X_c (%)
Neat LDPE	109.62 ± 0.42	74.46 ± 0.22	25.85 ± 0.08
MB10	109.67 ± 0.18	67.67 ± 0.26	25.99 ± 0.10
MB16	109.69 ± 0.21	60.28 ± 0.56	25.00 ± 0.23
MB25	109.53 ± 0.07	53.18 ± 0.25	25.14 ± 0.12
MB31	109.53 ± 0.12	46.46 ± 1.07	23.33 ± 0.54

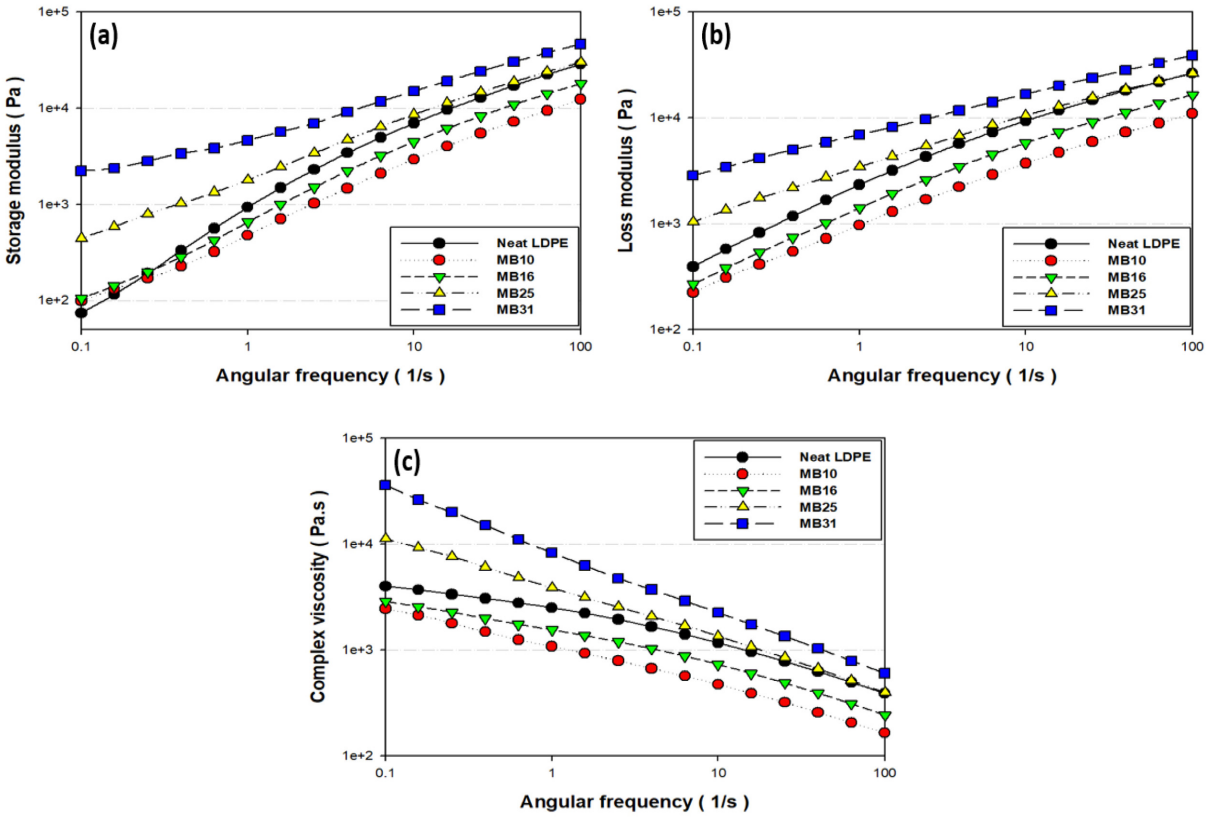

Fig. 1. (a) Storage modulus, *G'* (b) loss modulus, *G"*, (c) complex viscosity η^* of the LDPE/zeolite 4A composites.

crystalline region resulting from the lower ratio of LDPE. The crystallinity was also similar to that of neat LDPE, and it was confirmed that the increase of zeolite 4A content did not significantly affect the increase or decrease of crystallinity. However, when the amount of zeolite exceeds 31 wt%, the crystallinity was found to decrease slightly. The filler is mainly dispersed in the amorphous region of the polymer, but a large amount of the filler invades the crystalline region where crystallization occurs resulting the reduction of the crystallinity.

2. Rheological properties

The result of rotational rheometer analysis of LDPE/zeolite 4A composites are illustrated in Fig. 1 for evaluation of the modulus and complex viscosity in the molten state (200°C) to assess the effect of zeolite 4A content in LDPE. A trend of increasing *G', G"* and η^* as the addition of zeolite 4A to LDPE was observed.

When the zeolite content was less than 17 wt% in the LDPE matrix, it was observed that the complex viscosity was lower than that of neat LDPE. Generally, when the inorganic filler is dispersed in the polymer matrix, the complex viscosity increases depending on the content. It is necessary to apply a higher shearing force when dispersing the zeolite 4A in the LDPE matrix[29].

MB31 showed the plateau behavior at the low frequency region in the storage modulus curve. In addition, it was confirmed that the complex viscosity increases linearly with decreasing frequency showing the solid-like behavior. In case of the content of zeolite 4A was 25 wt% or more, the complex viscosity was higher than that of neat LDPE, and this could be

Table 3. Mechanical properties of LDPE/zeolite 4A composite films

Sample Code	Tensile strength (MPa)	Elongation at break (%)	Young's modulus (MPa)
Neat LDPE	13.89 ± 0.83	378.60 ± 30.65	116.02 ± 3.60
10F	8.63 ± 0.29	228.01 ± 15.29	125.56 ± 4.55
16F	8.97 ± 1.32	50.56 ± 5.74	154.07 ± 15.78
25F	8.01 ± 0.24	35.78 ± 3.93	195.52 ± 13.31
31F	6.99 ± 0.50	18.11 ± 1.89	206.93 ± 18.99

Table 4. Mechanical properties of LDPE/zeolite 4A composite foaming films

Sample Code	Tensile strength (MPa)	Elongation at break (%)	Young's modulus (MPa)
10FF	4.32 ± 0.11	63.78 ± 6.61	85.45 ± 2.59
16FF	4.02 ± 0.32	37.00 ± 4.64	68.29 ± 5.56
25FF	2.60 ± 0.20	9.53 ± 0.48	45.82 ± 4.40
31FF	2.69 ± 0.17	7.64 ± 0.55	39.31 ± 2.02

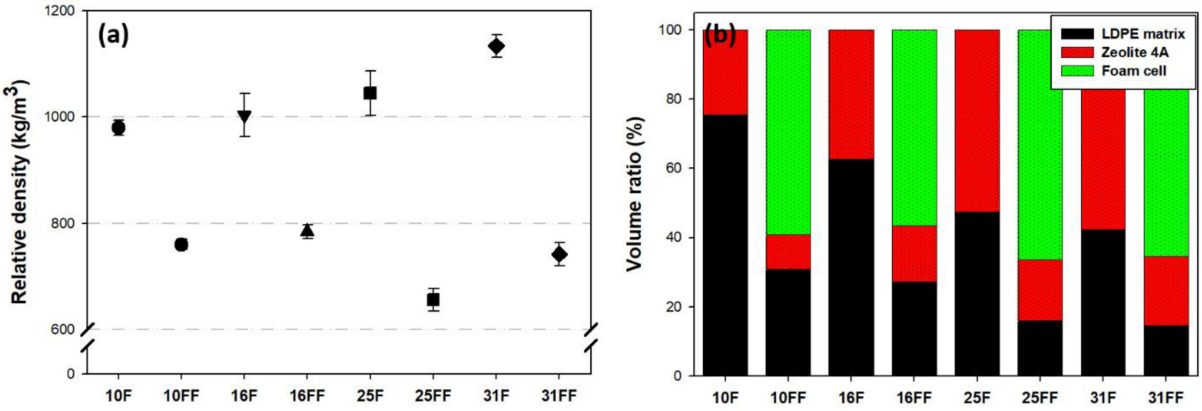

Fig. 2. (a) Relative density, (b) The volume ratio of the LDPE/zeolite 4A composite films (F series) and the foaming films (FF series).

due to that the filler was concentrated in the amorphous region, and the molecular chain mobility could be reduced.

3. Mechanical properties

Table 3 shows the mechanical properties of LDPE/zeolite 4A composite films and foaming films. As the content of zeolite 4A in LDPE matrix increases in both composite films and foam films, tensile strength and elongation at breaks was found to decrease. Composite films with 10 wt% zeolite 4A in LDPE matrix showed 37.8% decrease in tensile strength and 40% decrease in elongation at break, and this could be due to the lack of interfacial adhesion between the polymer matrix and the filler[27]. As the filler content increased, the young's modulus of the composite films increased. The increase in the Young's modulus of the zeolite 4A composite film indicates an increase in the stiffness of the LDPE associated with the limitation of the mobility of the LDPE matrix due to the presence of the filler[32].

The mechanical properties of the foaming film are shown in Table 4. Similarly to the composite films, the mechanical properties are decreased due to the increase of the content of zeolite 4A in polymer matrix. As the foam cells are created in the LDPE matrix, the interfacial adhesion area between the polymers is decreased resulting the reduction of young's modulus. In addition, as the content of zeolite increases, the adhesion surface area of the polymer matrix to each other is further reduced, resulting in the reverse synergy effect. Therefore, under the conditions of the same content of the filler, the foaming film tends to have lower mechanical properties such as tensile strength, elongation at break and young's modulus as compared with the composite film.

4. Physical properties

The main advantage of the foaming process is the reduction in density. In Fig. 2, the density of the foaming films is reduced by 22 to 37% as compared with the composite films. Given the calculation followed by Eqs. (3) and (4), LDPE matrix, zeolite 4A and air cell is calculated. Theoretical calculations confirmed that between 56 and 66% of foam cells per volume were created in the polymer matrix due to 10 phr

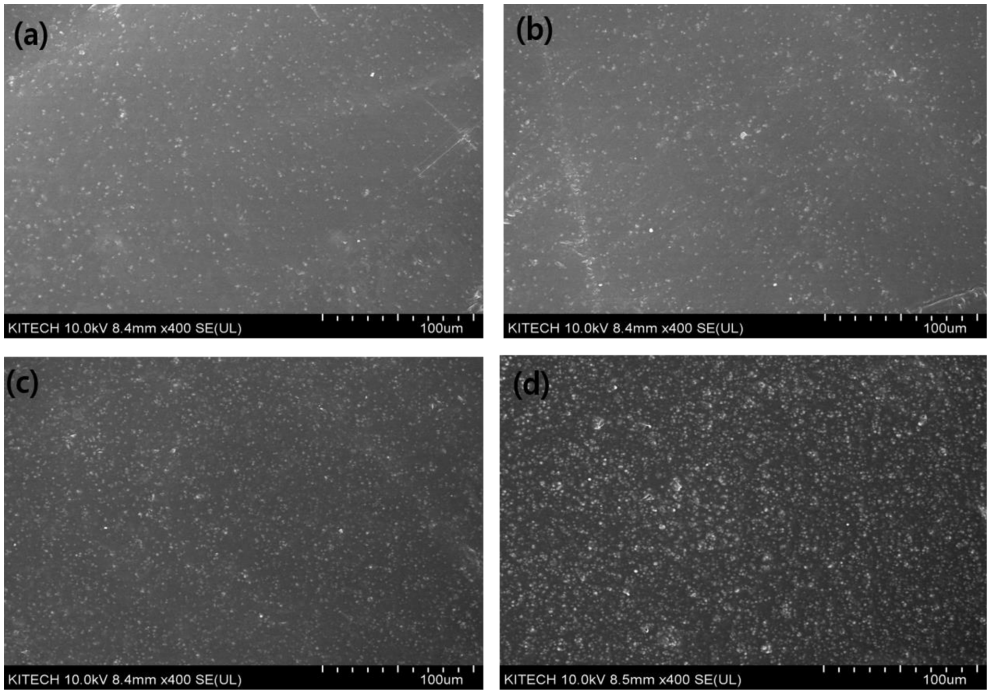

Fig. 3. SEM images of LDPE/zeolite 4A composite films surface with different zeolite 4A weight ratio; (a) 10F, (b) 19F, (c) 25F, (d) 31F.

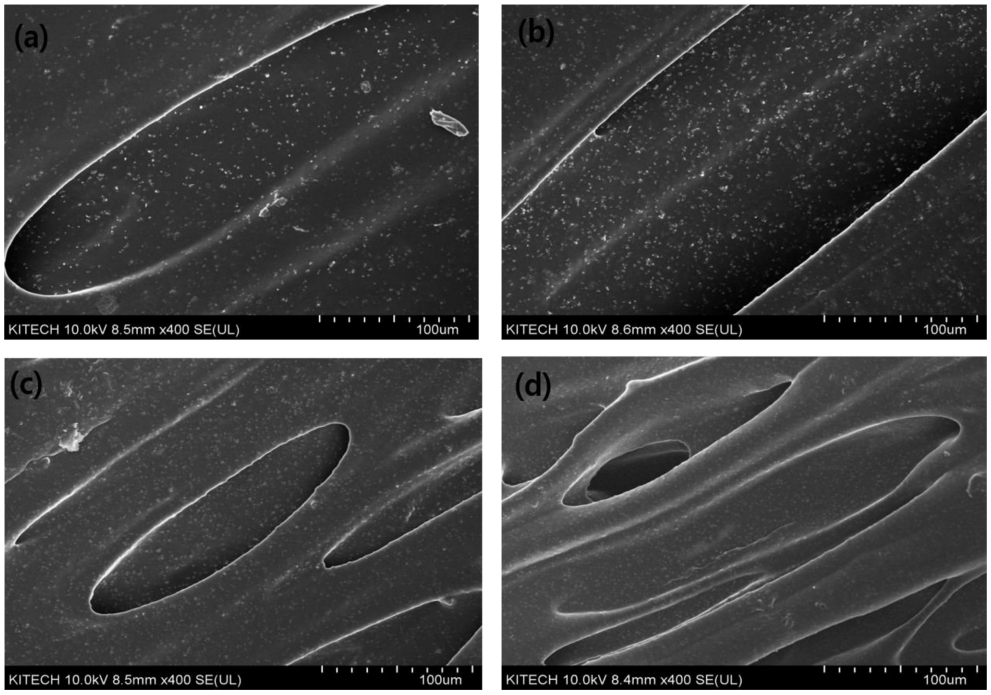

Fig. 4. SEM images of LDPE/zeolite 4A composite foaming films surface with different zeolite 4A weight ratio; (a) 10FF, (b) 19FF, (c) 25FF, (d) 31FF.

of blowing agent. The difference in the volume ratio of the foamed cells is due to the content of zeolite 4A. It could be seen in Fig. 1 that the complex viscosity at the low frequency region is significantly higher than the neat LDPE in the case of the zeolite content of 25 wt% or more. As a result, the foaming agent is not easily dispersed resulting in the aggre-

gation phenomenon. The difference in relative density was observed due to the difference in the size of the foam cell as confirmed in Fig. 5.

5. Morphological properties

Figs. 3 and 4 show a SEM image of the LDPE/zeolite 4A composite film and foaming film samples. On the surface of the films, it was observed that the zeolite was uniformly dispersed well in the LDPE matrix regardless of the content of the filler. The SEM results also confirm that the number of cells on the surface increases as the content of zeolite 4A increases on the surface of the foaming film.

Fig. 5 shows the cross section images of the foaming films. As the content of zeolite 4A increases, the size of the foam cell becomes uneven and larger. It could be seen that the surface of the foaming film affects the roughness according to the content of the filler. This is due to the non-uniform dispersion of the blowing agent due to the high complex viscosity (η^*) in the LDPE/zeolite 4A M/B molten state with increasing filler content as observed in Fig. 1.

6. Carbon dioxide adsorption properties

Fig. 6 (a) shows the CO_2 adsorption results of the LDPE/zeolite 4A composite films, and (b) foaming films. In this adsorption plots, Langmuir isotherms that occur in solid physical adsorption are observed. As seen in Fig. 6(a), the adsorption performance is gradually improved according to the content of zeolite 4A. 31F shows the highest value with adsorption amount of about 18 cc/g_{resin}. This adsorption takes place by zeolite 4A, which is evenly dispersed in the LDPE matrix, as shown in Figs. 3 and 4. Firstly, adsorption occurs on the zeolite 4A dispersed on the surface. Then, CO_2 is adsorbed on the inside of the film and adsorbed on the zeolite 4A dispersed in the film, and finally the adsorption equilibrium is obtained.

However, the foaming film was analyzed to have lower CO_2 adsorption than the composite film. In particular, when the content of zeolite 4A was 16 wt% or less, the adsorption performance was measured very poorly. Gases such as CO_2, nitrogen, ammonia and the like are released to decompose the chemical blowing agent to form a foaming cell. At this time, the generated gas adsorbs to the zeolite 4A while forming the cell. The adsorption efficiency decreases when zeolite is repeatedly adsorbed and desorbed.[33] Therefore, it could be inferred that such decrease in adsorption performance occurred in this study.

However, the foaming film has a faster time to reach the adsorption equilibrium and a higher adsorption rate than the composite film. This depends on two factors. First, as shown in Fig. 5, the foaming film has a rougher film surface than the composite film. Thus, the surface area is relatively large, which causes the adsorption reaction to take place actively on the surface. Secondly, due to the cells generated inside the film, the CO_2 can be more easily adsorbed inside the film, which results in adsorption equilibrium in a relatively short time.

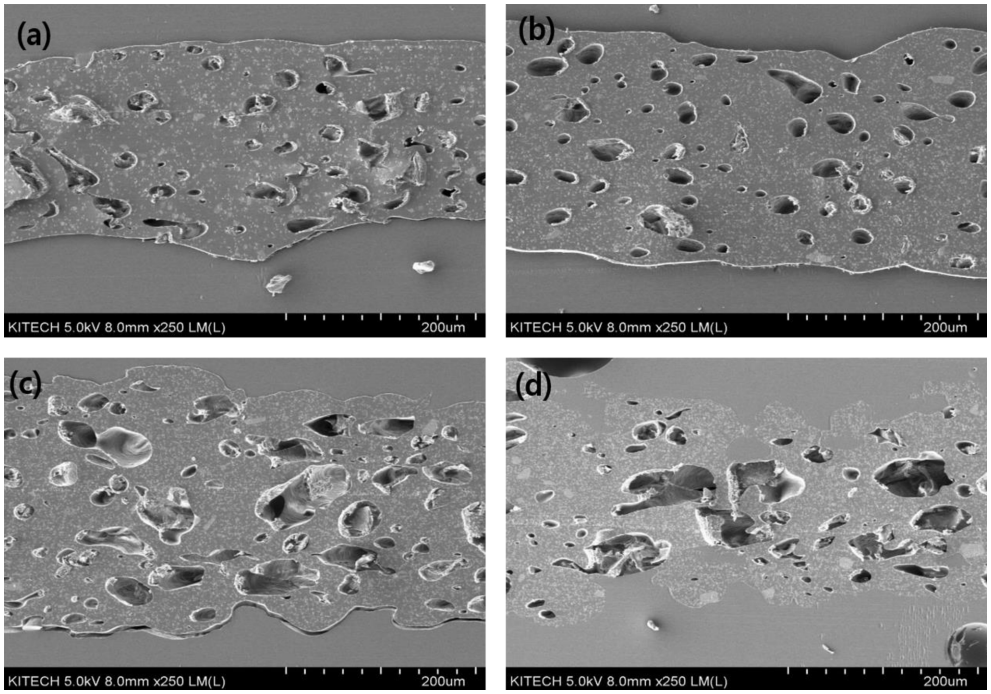

Fig. 5. SEM images of LDPE/zeolite 4A composite foaming films cross section with different zeolite 4A weight ratio; (a) 10FF, (b) 19FF, (c) 25FF, (d) 31FF.

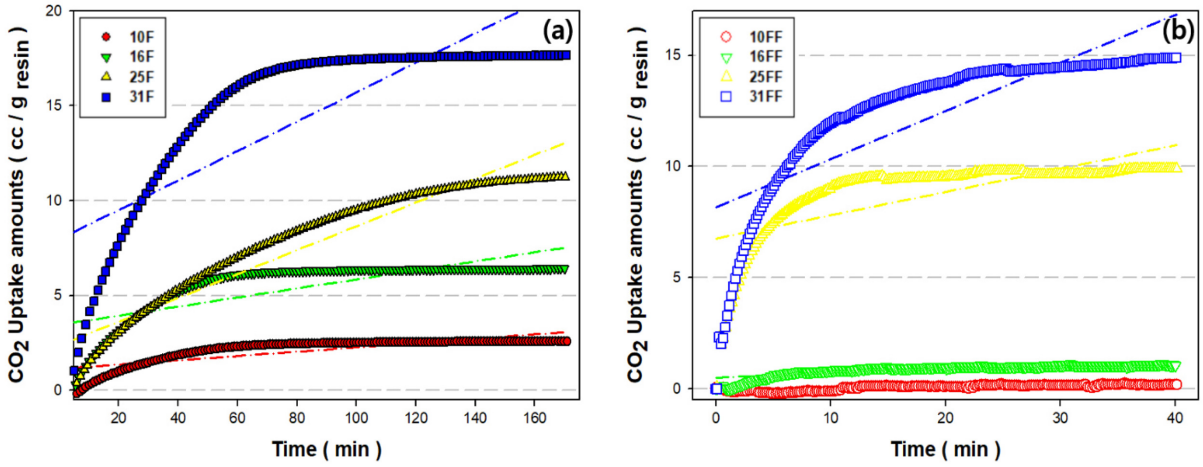

Fig. 6. CO_2 adsorption properties of LDPE/zeolite 4A composite (a) films and (b) foaming films.

Resulting in increasing of the CO_2 adsorption amounts due to increase of zeolite 4A content in the LDPE matrix. Therefore, the CO_2 adsorption properties could be controlled by the weight fraction of zeolite 4A in composite system, and could be achieved the optimized adsorption properties such as adsorption amount and rate depending on the active packaging application such as high and low CO_2 adsorption requirement for packaging industry.

Conclusions

The LDPE/zeolite 4A composite master batches were prepared by varying the contents of zeolite 4A in LDPE with a melt process method. Then, the composite film (F series) was extruded using a master batch, and 10 phr of a chemical blowing agent was added to prepare a foamed film (FF series). In thermal properties, there was no significant difference in the degree of crystallinity depending on the content of zeolite 4A. However, when the content of zeolite was more than 31 wt%, it showed decrease tendency slightly. The complex viscosity gradually increased with the content of zeolite 4A, and this increase was also confirmed from the SEM analysis to adversely affect the morphogenesis of foamed cells. In mechanical properties, as the content of zeolite 4A in LDPE matrix increases in both composite films and foaming films, tensile strength and elongation at breaks tended to decrease. The foaming film was found to have lower mechanical properties such as tensile strength, elongation at break and young's modulus as compared with the composite film. However, due to the chemical foaming, the relative density decreased as compared to the composite film. Based on the results of physical analysis, about 22~37% reduction of relative density is achieved with 10 phr of blowing agent compared to composite film. The CO_2 adsorption performance is gradually improved according to the content of zeolite 4A. It was found that the foaming film showed a faster time to reach the adsorption equilibrium and a faster adsorption rate than the composite film. By manufacturing LDPE/zeolite 4A composite film and foaming film using continuous extrusion process with excellent productivity, LDPE/zeolite 4A could be applied in fields requiring the balanced properties of various CO_2 adsorption active packaging applications by controlling composition of the composites.

Acknowledgement

This research is financially supported by the Rural Development Administration in South Korea (Project number: PJ01 3527).

References

1. Selke, S. E. and Culter, J. D. 2016. Plastics packaging: Properties, processing, applications, and regulations. Carl Hanser Verlag GmbH Co KG, Germany.
2. Daniels, J. A., Krishnamurthi, R., and Rizvi, S. S. 1985. A review of effects of carbon dioxide on microbial growth and food quality. J. Food Prot. 48: 532-537.
3. Sørheim, O., Ofstad, R., and Lea, P. 2004. Effects of carbon dioxide on yield, texture and microstructure of cooked ground beef. Meat Sci. 67: 231-236.
4. Luno, M. A., Beltrán, J., and Roncalés, P. 1998. Shelf-life extension and colour stabilisation of beef packaged in a low O_2 atmosphere containing CO: Loin steaks and ground meat. Meat Sci. 48: 75-84.
5. Fu, S.-Y., Feng, X.-Q., Lauke, B., and Mai, Y.-W. 2008. Effects of particle size, particle/matrix interface adhesion and particle loading on mechanical properties of particulate-polymer composites. Compos. B Eng. 39: 933-961.
6. Cavenati, S., Grande, C. A., and Rodrigues, A. E. 2004.

Adsorption equilibrium of methane, carbon dioxide, and nitrogen on zeolite 13X at high pressures. J. Chem. Eng. Data. 49: 1095-1101.
7. Saha, D., Bao, Z., Jia, F., and Deng, S. 2010. Adsorption of CO_2, CH_4, N_2O, and N_2 on MOF-5, MOF-177, and zeolite 5A. Environ. Sci. Technol. 44: 1820-1826.
8. Zhao, Z., Cui, X., Ma, J., and Li, R. 2007. Adsorption of carbon dioxide on alkali-modified zeolite 13X adsorbents. Int. J. Greenh. Gas Con. 1: 355-359.
9. Ko, D., Siriwardane, R., and Biegler, L. T. 2003. Optimization of a pressure-swing adsorption process using zeolite 13X for CO_2 sequestration. Ind. Eng. Chem. Res. 42: 339-348.
10. Chue, K., Kim, J., Yoo, Y., Cho, S., and Yang, R. 1995. Comparison of activated carbon and zeolite 13X for CO_2 recovery from flue gas by pressure swing adsorption. Ind. Eng. Chem. Res. 34: 591-598.
11. Lu, C., Bai, H., Wu, B., Su, F., and Hwang, J. F. 2008. Comparative study of CO_2 capture by carbon nanotubes, activated carbons, and zeolites. Energy Fuels 22: 3050-3056.
12. Zhao, J., Buldum, A., Han, J., and Lu, J. P. 2002. Gas molecule adsorption in carbon nanotubes and nanotube bundles. Nanotechnology 13: 195.
13. Park, I.-G., Hong, M.-S., Kim, B.-S., and Kang, H.-G. 2013. Ambient CO_2 adsorption and regeneration performance of zeolite and activated carbon. J. Korean Soc. Environ. Eng. 35: 307-311.
14. Siriwardane, R. V., Shen, M.-S., Fisher, E. P., and Poston, J. A. 2001. Adsorption of CO_2 on molecular sieves and activated carbon. Energy Fuels 15: 279-284.
15. Cooksey, K. 2001. Antimicrobial food packaging materials. Additives for Polymers 2001: 6-10.
16. Mengeloglu, F. and Matuana, L. M. 2001. Foaming of rigid PVC/wood-flour composites through a continuous extrusion process. J. Vinyl Addit. Techn. 7: 142-148.
17. Li, Q. and Matuana, L. M. 2003. Foam extrusion of high density polyethylene/wood-flour composites using chemical foaming agents. J. Appl. Polym. Sci. 88: 3139-3150.
18. Matuana, L. M. and Mengeloglu, F. 2001. Microcellular foaming of impact-modified rigid PVC/wood-flour composites. J. Vinyl Addit. Techn. 7: 67-75.
19. Libby, B., Smyrl, W., and Cussler, E. 2003. Polymer-zeolite composite membranes for direct methanol fuel cells. AIChE J. 49: 991-1001.
20. Süer, M. G., Baç, N., and Yilmaz, L. 1994. Gas permeation characteristics of polymer-zeolite mixed matrix membranes. J. Memb. Sci. 91: 77-86.
21. Byun, S. C., Jeong, Y. J., Park, J. W., Kim, S. D., Ha, H. Y., and Kim, W. J. 2006. Effect of solvent and crystal size on the selectivity of ZSM-5/Nafion composite membranes fabricated by solution-casting method. Solid State Ion. 177: 3233-3243.
22. Huang, Z., Shi, Y., Wen, R., Guo, Y.-H., Su, J.-F., and Matsuura, T. 2006. Multilayer poly (vinyl alcohol)-zeolite 4A composite membranes for ethanol dehydration by means of pervaporation. Sep. Purif. Technol. 51: 126-136.
23. Pechar, T. W., Kim, S., Vaughan, B., Marand, E., Tsapatsis, M., Jeong, H. K., and Cornelius, C. J. 2006. Fabrication and characterization of polyimide-zeolite L mixed matrix membranes for gas separations. J. Memb. Sci. 277: 195-202.
24. Ge, Q., Wang, Z., and Yan, Y. 2009. High-performance zeolite NaA membranes on polymer-zeolite composite hollow fiber supports. J. Am. Chem. Soc. 131: 17056-17057.
25. Chen, Z., Holmberg, B., Li, W., Wang, X., Deng, W., Munoz, R., and Yan, Y. 2006. Nafion/zeolite nanocomposite membrane by in situ crystallization for a direct methanol fuel cell. Chem Mater. 18: 5669-5675.
26. Wang, H., Holmberg, B. A., and Yan, Y. 2003. Synthesis of template-free zeolite nanocrystals by using in situ thermoreversible polymer hydrogels. J. Am. Chem. Soc. 125: 9928-9929.
27. Metın, D., Tihminlioğlu, F., Balköse, D., and Þlkü, S. 2004. The effect of interfacial interactions on the mechanical properties of polypropylene/natural zeolite composites. Compos. Part A Appl. Sci. Manuf. 35: 23-32.
28. Han, B., Wang, X., Sun, Z., Yang, J., and Lei, Q. 2013. Space charge suppression induced by deep traps in polyethylene/zeolite nanocomposite. Appl. Phys. Lett. 102: 012902.
29. Kim, H., Biswas, J., and Choe, S. 2006. Effects of stearic acid coating on zeolite in LDPE, LLDPE, and HDPE composites. Polymer 47: 3981-3992.
30. Wunderlich, B. 2012. Macromolecular physics vol 2. Elsevier, Netherlands.
31. Bonenfant, D., Kharoune, M., Niquette, P., Mimeault, M., and Hausler, R. 2008. Advances in principal factors influencing carbon dioxide adsorption on zeolites. Sci. Technol. Adv. Mater. 9: 013007.
32. Guerrica-EchevarríA, G., Eguiazabal, J., and Nazabal, J. 1998. Influence of molding conditions and talc content on the properties of polypropylene composites. Eur. Polym. J. 34: 1213-1219.
33. Wang, S., Li, H., Xie, S., Liu, S., and Xu, L. 2006. Physical and chemical regeneration of zeolitic adsorbents for dye removal in wastewater treatment. Chemosphere. 65: 82-87.

투고: 2018.11.13 / 심사완료: 2018.12.28 / 게재확정: 2018.12.28